Objective

The goal here is to summarize the possible modelisations of the SLM process, associated with metallic powder bed additive manufacturing processes. While the laser is moving along the scanning path, different phenomena occur. Figure 1. The aim of this paper is to sketch the main ones in order to choose a simplified model on which working.

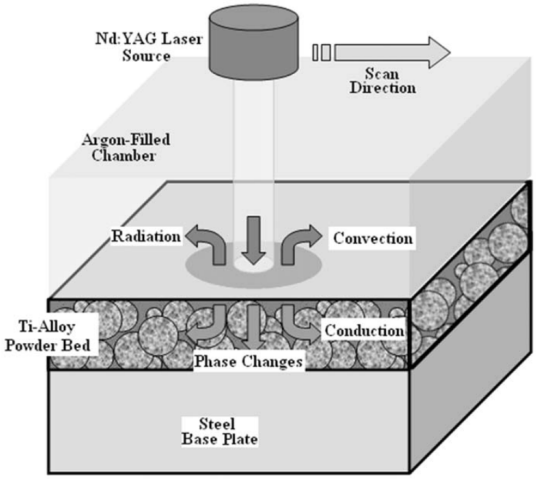

Figure 1: Schematic representation of heat transfer [5]

These phenomena have different effects on the process and can be split into two main groups : microscopic (focusing on the melting pool and the phase changement) and macroscopic (considering phenomena at the scale of the complete layer to build). A mesoscopic approach can then be run to link the two previous ones. ([4, 6])

1 Microscopic phenomena

The information about this part are mainly driven from [2, 4] The microscopic model aims at representing what happends in the melting pool. The domain taken for this study is of a size comparable to the melting pool's one. In this model are considered :

- heat source interaction with the feedstock,
- heat transfer (with high convection and radiation in the liquid phase),
- phase change (thermic parameters are modified depending on the temperature),
- surface tension forces,
- effect of thermal gradients leading to Marangoni forces,
- buoyancy.

1.1 Model equations

The notations here are ρ the fluid density, t is time, $\vec{\nu}$ the mass-averaged velocity vector, p the hydrodynamic pressure, τ the deviatoric shear stress, C a large constant, f_L the liquid fraction and f_v the vapor fraction while the phase is changing, σ the surface tension, κ the surface curvature, $\vec{n}$ the normal vector, T the temperature, p_R the recoil pressure, $\vec{g}$ the gravity vector, h the total enthalpy and h_i the specific enthalpy for the species i, λ the conductivity, $\vec{j_i}$ the species mass flux, L_f and L_v the latent heat of fusion and evaporation, S_r the term source representing radiation, Y_i the species mass fraction, m_L and m_v the liquid and vapor mass sources due to phase change.

Different phenomena have to be modelised (equations from [4]):

- Mass conservation :

$$\partial_t \rho + \nabla . \rho \vec{\nu} = 0 \tag{1}$$

- Momentum conservation :

$$\partial_t(\rho\vec{\nu}) + \nabla.\rho\vec{\nu}\vec{\nu} = -\nabla p + \nabla.\tau - \frac{C(1-f_L)^2}{f_L^3 + 10^{-10}}\vec{\nu} + \Big[\sigma\kappa\vec{n} + \frac{d\sigma}{dT}\Big(\nabla T - \vec{n}(\vec{n}.\nabla T)\Big)\Big] \cdot \vec{n} + p_R \cdot \vec{n} + \rho\vec{g} \tag{2}$$

- Energy conservation :

$$\partial_t(\rho h) + \nabla.\rho\vec{\nu}h = \nabla.\Big(\lambda\nabla T + \sum_i h_i\vec{j_i}\Big) + \partial_t p + \tau : \nabla\vec{\nu} - \partial_t(\rho f_L L_f) - \nabla(\rho\vec{\nu}f_L L_f) - \rho\partial_t((1-f_v)L_v) + S_R \cdot \vec{n} \tag{3}$$

- Species conservation :

$$\partial_t(\rho Y_i) + \nabla.\rho\vec{\nu}Y_i = \nabla.\vec{j_i}, \quad \forall i \in [\![1, N_{sp}]\!] \tag{4}$$

- Equation to track the free surface of the molten metal :

$$\partial_t\alpha_L + \nabla.\alpha_L\vec{\nu} = \frac{m_L}{\rho_L} - \frac{m_v}{\rho_L} \tag{5}$$

These equations can be simplified with some hypothesis. For exemple, in [2], they assume that there is no material losses by evaporation and that the liquid density stays constant in time. This lead to a new system of equations. (I haven't checked that they really correspond to the ones written above).

1.2 To control

Finally, let's explain why considering the microscopic scale is important. First of all, this enables a accurate description of the absorption of the heat source and thus gives an "equivalent" heat source for the macroscopic scale. Moreover, some defects come from the melting pool and the way the phase is changing. Some examples of these problems are presented here (see mainly [2]).

- Kevin Helmoltz instabilities
- Raleigh capillary instabilities
- loosing elements through evaporation
- porosity
- surface roughness
- damages...

2 Macroscopic phenomena

The macroscopic model "ignores" what happens in the melting pool. It considers more "global" effects and the domain size is the workingpiece one. The goal of this approach is to determine the residual stresses and distortion happening at the scale of the workpiece. To get this, a "two-scale" model is developed : first a heat transfer model whose results will be used for a mechanical analysis.

2.1 Heat transfer analysis

In this model are considered :

- the absorption of the heat source (modelized to void considering the melting pool)
- conduction in the solid
- radiation and convection

It is also assumed that the thermic parameters are constant over time and they don't depend on temperature but only of the fact that the represent powder or solid.

Model equations

We note ρ, λ, h, T, Q respectively the density, the conductivity, the enthalpy, the temperature and the inter volumic heat source. The parameter c_p is the specific heat, that we assume constant over time (it only differs from solid to powder but the specific heat of powder and of solid stay constant over time). The ambiant temperature is T_0, $\beta(x)$ is the heat convection coefficient, A the Hooke's operator. Finally, α is the thermal expansion coefficient, $f_{VonMises}$ the yield function and σ_Y the yield stress.

The solid and the powder have different values for some physical parameters. Thus, we consider here (for example with χ_{solid} the solid characteristic, ρ_{solid} the density of the solid and rho_{powder} the density of the powder): ([3, 5, 1])

$$\begin{aligned}
\rho &= \rho_{solid} * \chi_{solid} + \rho_{powder} * (1 - \chi_{solid}) \\
c_p &= c_{p,solid} * \chi_{solid} + c_{p,powder} * (1 - \chi_{solid}) \\
\lambda &= \lambda_{solid} * \chi_{solid} + \lambda_{powder} * (1 - \chi_{solid}) \\
\epsilon &= \epsilon_{solid} * \chi_{solid} + \epsilon_{powder} * (1 - \chi_{solid}) \\
A &= A_{solid} * \chi_{solid} + A_{powder} * (1 - \chi_{solid}) \\
\beta &= \beta_{solid} * \chi_{solid} + \beta_{powder} * (1 - \chi_{solid})
\end{aligned} \tag{6}$$

The coefficient for the solid and the powder can sometimes be related (conductivity for example, considering the porousity of the powder).

- equations in the workpiece ([3, 5, 1, 4]):

$$\rho(x)\partial_t h(t,x) - \nabla(\lambda(x)\nabla T(t,x)) = Q, \qquad \forall (t,x) \in (0,t_F) \times D \tag{7}$$

Specific heat and enthalpy are linked by (with f_L the fraction of liquid and L_f the latent heat)

$$h = \int_{T_0}^{T} c_p(T)dT + f_L L_f \tag{8}$$

Since the melting pool is ignored here and that the thermi parameters are considered constant over time, we get :

$$\rho(x)\partial_t h(t,x) = \rho(x)c_p(x)\partial_t T(t,x) \tag{9}$$

Thus the resulting equation is :

$$\rho c_p \partial_t T - div(\lambda \nabla T) = Q \qquad \text{in } (0,t_F) \times D \tag{10}$$

- limit conditions ([3, 5, 4]):

$$\begin{cases} (\lambda \nabla T)n = q - q_c - q_r \text{ on } \partial D_N \\ T = T_0 \text{ on } \partial D_D \end{cases} \tag{11}$$

with q_c the heat convection (different from solid to powder), q_r the heat radiation (σ_B is the Stefan-Boltzman constant, ϵ is the emissivity), and q is the heat source, considered as Gaussian here (Ab is the absorptance, P the laser power and R the effective laser beam radius):

$$\begin{cases} q_c = \beta(T - T_0) \\ q_r = \sigma_B \epsilon (T^4 - T_0^4) \\ q = \frac{2AbP}{\pi R^2} exp\Big(- \frac{2r^2}{R^2} \Big) \end{cases} \tag{12}$$

and the initial condition

$$T(x,y,z,0) = T_0 \ \forall x \in D \tag{13}$$

These boundary conditions are sumed up in Figure 2:

This leads to the following thermic problem :

$$\begin{cases} \rho c_p \partial_t T - div(\lambda \nabla T) = Q & \text{in } (0,t_F) \times D \\ (\lambda \nabla T)n = q - \beta(T - T_0) - \sigma_B \epsilon (T^4 - T_0^4) & \text{on } (0,t_F) \times \partial D_N \\ T = T_0 & \text{on } (0,t_F) \times \partial D_D \\ T(x,y,z,0) = T_0 & \text{in } D \end{cases} \tag{14}$$

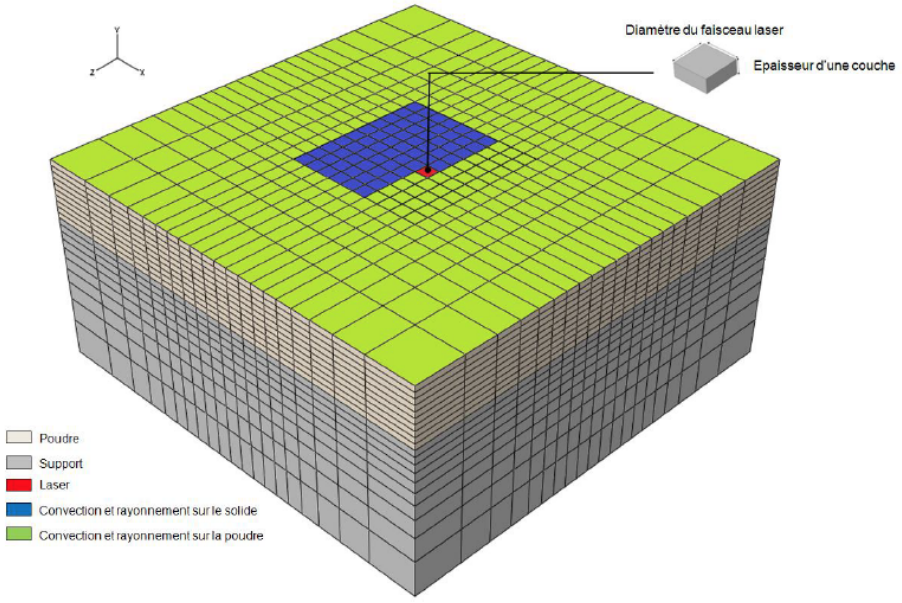

Figure 2

2.2 Thermo-mechanical analysis

The mechanical analysis is non-linear. Depending on the loading applied and on the thermal load resulting from the laser scanning, plasticity can occur. We consider here a quasistatic model ([4]) and the annealing effects are ignored.

Model equations

$$\begin{cases} \nabla.\sigma + \vec{f} = 0 \\ \epsilon^{tot} = \epsilon^e + \epsilon th + \epsilon^p \\ \sigma^e = C\epsilon^e = Ae(u^e) \\ \epsilon^{th} = \alpha(T - T_0) \\ \epsilon^p = f_{VonMises}(\sigma_Y) \end{cases} \tag{15}$$

Boundary conditions are added to the problem :

$$\begin{cases} \sigma\vec{n} = 0 & \text{on } \partial D_N \\ u = 0 & \text{on } \partial D_D \end{cases} \tag{16}$$

2.3 To control

Different variables have to be controlled ([2]):

- thermal stress : to avoid plasticity and thus residual constraints, the thermal stress must stay low.
- spatial thermic gradient : this one could also cause residual stresses and must be kept low too.

3 Model for now

A first model has been chosen to simplify the computation and to be taken as a working basis. This is basically the one taken in [1].

3.1 Model in 2D, for only one layer

$$\begin{cases} \rho c_p \partial_t T - div(\lambda \nabla T) + \lambda T = q_{source} & \text{in } (0, t_F) \times D \\ (\lambda \nabla T)n = -\beta(T - T_0) & \text{on } (0, t_F) \times \partial D_N \\ T = T_0 & \text{on } (0, t_F) \times \partial D_D \\ T(x, y, z, 0) = T_0 & \text{in } D \end{cases} \tag{17}$$

$$\begin{cases} -div(\sigma) = f & \text{in } (0, t_F) \times D \\ \sigma = \sigma^{el} + \sigma^{th} & \text{in } (0, t_F) \times D \\ \sigma^{el} = Ae(u) \quad \sigma^{th} = K(T - T_0)I_n & \\ \sigma.n = 0 & \text{on } (0, t_F) \times \partial D_N \\ u = 0 & \text{on } (0, t_F) \times D_D \end{cases} \tag{18}$$

3.2 Model in 3D, for more than one layer

References

[1] G. Allaire et L Jakabčin : Taking into account thermal residual stresses in topology optimization of structures built by additive manufacturing. décembre 2017.

[2] T. DebRoy, H. L. Wei, J. S. Zuback, T. Mukherjee, J. W. Elmer, J. O. Milewski, A. M. Beese, A. Wilson-Heid, A. De et W. Zhang : Additive manufacturing of metallic components – Process, structure and properties. *Progress in Materials Science*, 92:112–224, mars 2018.

[3] Yali Li et Dongdong Gu : Parametric analysis of thermal behavior during selective laser melting additive manufacturing of aluminum alloy powder. *Materials & Design*, 63:856–867, novembre 2014.

[4] Mustafa Megahed, Hans-Wilfried Mindt, Narcisse N'Dri, Hongzhi Duan et Olivier Desmaison : Metal additive-manufacturing process and residual stress modeling. *Integrating Materials and Manufacturing Innovation*, 5(1):4, décembre 2016.

[5] I. A. Roberts, C. J. Wang, R. Esterlein, M. Stanford et D. J. Mynors : A three-dimensional finite element analysis of the temperature field during laser melting of metal powders in additive layer manufacturing. *International Journal of Machine Tools and Manufacture*, 49(12):916–923, octobre 2009.

[6] Laurent Van Belle : *Analyse, Modélisation et Simulation de l'apparition de Contraintes En Fusion Laser Métallique*. Lyon, INSA, novembre 2013.